NEOPLASIA
www.neoplasia.com

Volume 15 Number 9 September 2013 pp. 1036–1048 1036

Tpl2 Inhibitors Thwart Endothelial Cell Function in Angiogenesis and Peritoneal Dissemination[1,2]

Wen-Jane Lee*,†, Keng-Hsin Lan‡,§,¶, Chiang-Ting Chou#, Yu-Chiao Yi, Wei-Chih Chen**, Hung-Chuan Pan¶,††, Yen-Chun Peng‡‡, Keh-Bin Wang§§, Yi-Ching Chen§§, Te-Hsin Chao¶¶, Hsing-Ru Tien##, Wayne Huey Herng Sheu##,††† and Meei-Ling Sheu*,##**

*Department of Education and Research, Taichung Veterans General Hospital, Taichung, Taiwan; †Department of Social Work, Tunghai University, Taichung, Taiwan; ‡Division of Gastroenterology, Department of Medicine, Taipei Veterans General Hospital, Taipei, Taiwan; §Department and Institute of Pharmacology, National Yang-Ming University, Taipei, Taiwan; ¶Department of Medicine, School of Medicine, School of Life Science, National Yang-Ming University, Taipei, Taiwan; #School of Nursing, Chang Gung University of Science and Technology, Chiayi, Taiwan; **Department of Obstetrics and Gynecology, Taichung Veterans General Hospital, Taichung, Taiwan; ††Department of Neurosurgery, Taichung Veterans General Hospital, Taichung, Taiwan; ‡‡Division of Gastroenterology, Department of Internal Medicine, Taichung Veterans General Hospital, Taichung, Taiwan; §§Department of Nuclear Medicine, Kuang Tien General Hospital, Taichung, Taiwan; ¶¶Division of Colorectal Surgery, Department of Surgery, Taichung Veterans General Hospital, Taichung, Taiwan; ##Institute of Biomedical Sciences, National Chung Hsing University, Taichung, Taiwan; †††Department of Internal Medicine, Taichung Veterans General Hospital, Taichung, Taiwan

Abstract

Angiogenesis is critical in the development of cancer, which involves several angiogenic factors in its peritoneal dissemination. The role of protein tumor progression locus 2 (Tpl2) in angiogenic factor–related endothelial cell angiogenesis is still unclear. To understand the precise mechanism(s) of Tpl2 inhibition in endothelial cells, this study investigated the role of Tpl2 in mediating angiogenic signals using *in vitro*, *in vivo*, and *ex vivo* models. Results showed that inhibition of Tpl2 inhibitor significantly reduced peritoneal dissemination in a mouse model

Abbreviations: Tpl2, tumor progression locus 2; PET/CT, positron emission tomography/computed tomography; VEGF, vascular endothelial growth factor; CXCL1, chemokine (C-X-C motif) ligand 1; bFGF, basic fibroblast growth factor; EGF, epidermal growth factor; C/EBPβ, CCAAT/enhancer binding protein β; NF-κB, nuclear factor κ light-chain enhancer of activated B cells; AP1, activating protein 1; HUVECs, human umbilical vein endothelial cells; SVECs, mouse microvascular endothelial cells

Address all correspondence to: Meei-Ling Sheu, PhD, Institute of Biomedical Sciences, College of Life Sciences, National Chung Hsing University, 250, Kuo Kuang Road, Taichung 402, Taiwan. E-mail: mlsheu@nchu.edu.tw or mlsheu99@yahoo.com.tw

[1]This study was supported by research grants from the National Science Council of Taiwan (NSC99-2320-B-005-003-MY3 and NSC102-2628-B-005-001-MY3); Taichung Veterans General Hospital in Taiwan (TCVGH-1017315C and TCVGH-1017322D). National Chung Hsing University (101S0515 and 102S0902).
[2]This article refers to supplementary materials, which are designated by Figures W1 and W2 and are available online at www.neoplasia.com.
Received 16 November 2012; Revised 5 February 2013; Accepted 13 May 2013

DOI 10.1593/neo.121914

by positron emission tomography/computed tomography imaging. Simultaneously, inhibiting Tpl2 blocked angiogenesis in tumor nodules and prevented angiogenic factor–induced proliferating cell nuclear antigen (PCNA) in endothelial cells. Vascular endothelial growth factor (VEGF) or chemokine (C-X-C motif) ligand 1 (CXCL1) increased Tpl2 kinase activity and phosphorylation in a dose- and time-dependent manner. Furthermore, Tpl2 inhibition or ablation by siRNA prevented the angiogenic signal–induced tube formation in Matrigel plug assay or aortic ring assay. Inhibiting Tpl2 also prevented the angiogenic factor–induced chemotactic motility and migration of endothelial cells. Tpl2 inhibition by CXCL1 or epidermal growth factor in endothelial cells was associated with inactivation of CCAAT/enhancer binding protein β, nuclear factor κ light-chain enhancer of activated B cells, and activating protein 1 and suppression of VEGF expression. Thus, Tpl2 inhibitors thwart Tpl2-regulated VEGF by inactivating transcription factors involved in angiogenic factor–triggered endothelial cell angiogenesis. These results suggest that the therapeutic inhibition of Tpl2 may extend beyond cancer and include the treatment of other diseases involving pathologic angiogenesis.

Neoplasia (2013) 15, 1036–1048

Introduction

The serine-threonine protein kinase encoded by the tumor progression locus 2 (Tpl2) proto-oncogene, also known as Cot, is a mitogen-activated protein kinase kinase kinase that is induced by Toll-like receptor, pro-inflammatory cytokines like tumor necrosis factor, and interleukin-1 in a variety of cell types [1–4]. Tpl2 is overexpressed in different types of malignancies like large granular lymphocyte proliferative disorders and human breast cancer [5,6]. The overexpression of Tpl2 in various cell types like colonic adenocarcinomas and gastric adenocarcinomas [7,8] and the activation of different mitogen-activated protein kinase pathways, nuclear factor–activated T cells, and nuclear factor κ light-chain enhancer of activated B cells (NF-κB), as well as the promotion of cell proliferation, have also been reported [2,3]. Previous studies suggest that the proteinase-activated receptor-1–triggered activation of Tpl2 promotes actin cytoskeleton reorganization and cell migration in stromal and tumor cells [9]. Suppressing Tpl2 diminishes the growth of androgen depletion–independent prostate cancer [10]. Recently, Tpl2 has been reported as a key mediator of arsenite-induced signal transduction of carcinogenesis in mouse epithelial cells [11]. Thus, Tpl2 is a critical component of the signaling pathway in tumor cells. Endothelial cell function is essential to tumor angiogenesis and peritoneal dissemination. However, the relevance of Tpl2 in angiogenic factor–induced angiogenesis associated with endothelial cells and the underlying mechanisms remain unclear.

Angiogenesis is critical in the development of cancer. The peritoneal dissemination of cancer is a process that involves several angiogenic factors, including vascular endothelial growth factor (VEGF), epidermal growth factor (EGF), basic fibroblast growth factor (bFGF), chemokine (C-X-C motif) ligand 1 (CXCL1), and other critical factors [12–16]. Of the various manifestations of the cancer progression, peritoneal dissemination is the most closely associated with poor operative results [17–20]. Blocked angiogenesis in tumors allows the anti-growth and anti-invasiveness of tumor cells leading to prevent peritoneal dissemination [12,18]. VEGF-mediated angiogenesis is associated with enhanced endothelial cell survival and induction of neovascularization. Recent reports have shown that blood vessels contain genetically normal and stable endothelial cells unlike tumor cells, which typically display genetic instability and are cytogenetically abnormal, suggesting that the tumor microenvironment contributes to these aberrations [21–23]. Therefore, anti-Tpl2 therapy represents one of the most promising approaches to stop the angiogenic process.

Several pathways have been involved in the angiogenesis induced by angiogenic growth factors. Emerging evidence shows that transcription factors are activated by phosphorylation and then translocated to the nucleolus that subsequently regulates angiogenesis [24]. Some of these [e.g., CCAAT/enhancer binding protein β (C/EBPβ), NF-κB, activating protein 1 (AP1), hypoxia-inducible transcription factor 1 alpha (HIF-1α), and specificity protein 1 (SP1)] bind to the VEGF promoter to initiate and activate the transcription of a gene directly. NF-κB is an important signal molecule associated with endothelial cell survival and migration induced by VEGF and bFGF [25–27]. A related activity factor C/EBPβ pathway activated by VEGF and bFGF has also been implicated in the regulation of cell motility and survival [28–30]. Specific knockdown of HIF-1α or Sp-1 *in vitro* leads to reduced expression of both VEGF and CXCL1 [31–35]. As such, the application of an anti-angiogenesis stratagem to control nuclear factor activation may be a promising approach for regulating angiogenesis, tumor growth, and metastasis. However, the molecular mechanisms by which Tpl2 regulates endothelial cell migration and tube formation are poorly understood.

The present study determined whether Tpl2 is necessary for endothelial cell growth signal transduction by investigating the angiogenic activities of Tpl2, including the promotion of a mouse model peritoneal dissemination *in vivo*, endothelial cell proliferation, migration and capillary tube formation of human umbilical vein endothelial cells (HUVECs) *in vitro*, and Matrigel plug assay *in vivo*. Because the inhibition of Tpl2 prevented vessel sprouting in an aortic ring assay *ex vitro*, the signaling pathways involved in angiogenesis mediated by Tpl2 were also investigated. Lastly, the transcription factors C/EBPβ, NF-κB, and AP1, the downstream effectors of Tpl2 for the mediation of VEGF expression, were also analyzed.

Materials and Methods

Chemicals and Reagents

Lipofectin reagent was obtained from Invitrogen (Life Technologies, Grand Island, NY). Specific Tpl2 inhibitor was purchased from

Calbiochem (San Diego, CA; Cat. No. 616373) [10,11]. The [γ-32P] adenosine triphosphate (ATP) was obtained from NEN (PerkinElmer, Waltham, MA). Tpl2 siRNA and antibodies for Tpl2, Ki67, and glyceraldehyde 3-phosphate dehydrogenase (GAPDH) were purchased from Santa Cruz Biotechnology (Santa Cruz, CA).

Cell Culture

HUVECs were obtained by collagenase treatment of umbilical cord veins as described previously [36]. HUVECs from the third passage were used, and the efficiency of transfection (>80%) by Lipofectin reagent (Invitrogen) was determined at the third passage. In some experiments, SV-40 immortalized mouse microvascular endothelial cells (SVECs) were cultured in Dulbecco's modified Eagle's medium Mixture F-12 supplemented with 10% FBS and 1% penicillin/streptomycin/amphotericin B. The ethics review board of Taichung Veterans General Hospital approved this study, which conforms to the Declaration of Helsinki for use of human tissue (Approval Document CE-12062).

Mouse Model of Animal Peritoneal Dissemination

All animal care and experimental procedures were approved and conducted by the Committee for Animal Experiments of National Chung Hsing University (Approval Document NCHU-100-26). Four- to six-week-old male BALB/c nude mice were purchased from National Laboratory Animal Center (NLAC; Taipei, Taiwan). The mice were bred and maintained under specific pathogen-free conditions, provided with sterilized food and water *ad libitum*, and housed in a barrier facility with a 12-hour light/dark cycle.

Xenograft Tumor Mouse Model

In the peritoneal metastasis model, cultured human gastric cancer cells (4×10^6 to 5×10^6 cells) were inoculated into the peritoneal cavity of BALB/c nude mice. MKN45 and SCM-1, undifferentiated adenocarcinoma cells, were obtained from the cell bank of Taipei Veterans General Hospital (Taipei, Taiwan). Positron emission tomography/computed tomography (PET/CT) was conducted 7 days after the intraperitoneal inoculation to confirm where the tumor has grown substantially in the abdominal cavity. If the tumor was successfully inoculated, the mice were injected intraperitoneally with Tpl2 inhibitor (2 mg/kg, twice per week). Serial surveillance PET/CT images from 14, 28, and 49 days after treatment with Tpl2 inhibitor were used to detect peritoneal dissemination. The mice were sacrificed under anesthesia (pentobarbital) and examined macroscopically for the presence of peritoneal metastasis. The tumors were excised, cut into blocks, fixed in 10% formalin, and embedded in paraffin blocks or snap-frozen in liquid nitrogen.

PET/CT Scanning

After at least 6 hours of fasting, the mice were given a 7.4-MBq (0.2-mCi) dose of ^{18}F-FDG orally before flushing with 1 ml of water. The mice were anesthetized with an isoflurane vaporizer before each scan. Experiments for small animal imaging were performed with a combined PET/CT scanner (Discovery ST; GE Medical Systems, Taichung, Taiwan). A multidetector row helical CT scanner was used. Technical parameters used in the CT portion of PET/CT were given as follows: CT scan type with a 0.5-second full helical scan; detector row configuration, 1661.25 mm; interval space, 2.75 mm; slice thickness, 1.25 mm; pitch, 1.75:1 (high-quality mode); speed, 17.5 mm per rotation; large field of view (FOV); voltage, 120 kVp; current, 200 mA. Technical parameters used for the PET portion of PET/CT included 10.0 minutes in each bed. The FOV chosen for imaging reconstruction was 20 cm with PET resolution of about 4.5-mm full width at half maximum. The reconstructive parameters were type 3D iteration as 21 subsets and two iterations. To evaluate the quantification ability of the PET/CT scanner in small animal imaging, a region of interest was placed on smaller FOV transaxial PET images to completely surround the areas of FDG uptake in the observed tissues while avoiding nearby tissues. The mean of each pixel's activity value within each region of interest was recorded and expressed as kBq/ml.

Immunohistochemistry

Assay was performed as previously described [18]. The expressions of CD31 proteins in mouse solid tumors were examined by immunohistochemistry. All tumors were fixed in 10% buffered formalin immediately after the animals were sacrificed. After pressure cooker pretreatment in citrate buffer (pH 6.0) for 30 minutes, 5-μm sections of the tumors were incubated at room temperature for 1 hour with a monoclonal antibody for CD31 (1:500; Santa Cruz Biotechnology). After incubation with an appropriate primary antibody enhancer, the slides were incubated with HRP polymer (Laboratory Vision Corporation, Fremont, CA). Staining was evaluated by two independent observers. For negative controls, primary antibodies were replaced by phosphate-buffered saline (PBS). For quantization of mean vessel density (MVD) in section, quantities were calculated as CD31-positive area/total area. Reaction products were visualized by immersing the slides in peroxidase-compatible chromogen. The slides were counterstained with hemalaun.

Measurement of Cell Proliferation

Cell proliferation was measured using the CellTiter 96 AQueous cell viability assay kit as described previously [37]. The assay was composed of the tetrazolium compound 3,4-(5-dimethylthiazol-2-yl)-5-(3-carboxymethoxyphenyl)-2-(4-sulfophenyl)-2H-tetrazolium salt (MTS) and an electron coupling reagent, phenazine methosulfate. MTS was reduced by viable cells to formazan, which could be measured with a spectrophotometer by the amount of 490-nm absorbance. Cultures were seeded at 1×10^4 cells/well and allowed to attach overnight. After incubation with the appropriate medium, 20 μl of MTS/phenazine methosulfate mixture was added per well and the cells were incubated for 1 hour before absorbance at 490 nm was measured. Background absorbance from the control wells was subtracted. Four duplicate studies were performed for each experimental condition.

Tpl2 Immunoprecipitation and Kinase Assay

The kinase activity was assessed as previously described with some modifications [11]. Cells were cultured to 80% confluence and then serum-starved in 0.1% FBS–minimum essential medium for 24 hours at 37°C. The cells were treated with pro-angiogenic factors for different periods as indicated, disrupted with lysis buffer [20 mM Tris-HCl (pH 7.4), 1 mM EDTA, 150 mM NaCl, 1 mM EGTA, 1% Triton X-100, 1 mM H-glycerophosphate, 1 mg/ml leupeptin, 1 mM Na_3VO_4, and 1 mM PMSF], and finally centrifuged at 20,000*g* for 10 minutes in a microcentrifuge. Lysates containing 500 to 1000 μg of protein were used for immunoprecipitation with antibody against Tpl2 and then incubated at 4°C overnight. After the addition of protein G Plus agarose beads, the mixture was continuously

rotated at 4°C. The beads were washed three times with kinase buffer [20 mM MOPS (pH 7.2), 25 mM H-glycerophosphate, 5 mM EGTA, 1 mM Na_3VO_4, and 1 mM DTT], resuspended in 20 μl of 1× kinase buffer, and incubated for another 30 minutes at 30°C. Then, 20 μg of myelin basic protein and 10 μl of diluted [γ-^{32}P] ATP solution were added, and the mixture was incubated for 10 minutes at 30°C. A 20-μl aliquot was transferred onto p81 paper and washed three times with 0.75% phosphoric acid for 5 minutes per wash, followed by a single wash with acetone for 2 minutes. The radioactive incorporation was determined using a scintillation counter. The experiments were done in triplicate.

Luciferase Reporter Assay

Endothelial cells at 60% confluence were co-transfected with 0.2 μg of the promoter-reporter construct C/EBPβ, NF-κB, and AP1 and 0.1 μg of a thymidine kinase promoter–driven renilla-luciferase vector (pRLTK; Promega, Mannheim, Germany). After 36 hours, the cells were lysed and processed using the Dual Luciferase Kit (Promega) as described by the manufacturer. Luciferase activity was normalized to renilla firefly activity for transfection efficiency and measured by a luminometer (LKB, Rockville, MD).

Tube Formation Assay

Assay was performed as previously described [18]. Matrigel was thawed at 4°C overnight, and each well of prechilled 48-well plates was coated with 100 μl of Matrigel and incubated at 37°C for 60 minutes. HUVECs (4×10^4 cells) were added to 1 ml of endothelial cell growth medium (ECGM) with various concentrations of Tpl2 inhibitor. After 12 hours of incubation at 37°C and 5% CO_2, endothelial cell tube formation was assessed using a Nikon inverted microscope with attached digital camera. Tubular structures were quantified by manual counting under low-power fields, and the inhibition percentage was expressed using untreated wells as 100%.

Ex Vivo *Vessel Sprouting Aortic Ring Assay*

Assay was performed as previously described [18]. Aortas were isolated from 6-week-old Sprague-Dawley rats. Plates (48-well) were coated with 120 μl of Matrigel. Aortas isolated from mice were cleaned of periadventitial fat and connective tissues and cut into 1- to 1.5-mm-long rings. After rinsing five times with endothelial cell–based medium, the aortas were placed on the Matrigel-coated wells and covered with another 100 μl of Matrigel. Tpl2 inhibitor or vehicle was added to the wells in a final volume of 250 μl of medium. Cultures were incubated, and media were replaced every second day over the course of the 8 to 10 days of experiments. Visual counts of microvessel outgrowths from replicate explant cultures ($n = 4$) were done under bright-field microscopy following an established protocol. Experiments were performed at least four times, and microvessel counts in treated and control cultures were analyzed.

Endothelial Cell Migration Assay

The chemotactic motility of HUVECs was assayed using Transwell (Corning Costar, Cambridge, MA) with 6.5-mm diameter polycarbonate filters (8-μm pore size) as described previously [18]. Briefly, the lower surface of the filter was coated with 10 μg of gelatin type B. Fresh M199 medium (1% FBS) containing VEGF was placed in the lower wells. Cells were trypsinized and suspended in a final concentration of 1×10^6 cells/ml in M199 containing 1% FBS. Various concentrations of Tpl2 inhibitor were given to the cells for 60 minutes at room temperature before seeding. One hundred microliters of the cell suspension was loaded into each of the upper wells. The chamber was incubated at 37°C for 4 hours. Cells were fixed and stained with hematoxylin and eosin (H&E). Nonmigrating cells on the upper surface of the filter were removed by wiping with a cotton swab. Chemotaxis was quantified by counting the cells that migrated to the lower side of the filter with an optical microscope (×200). Ten fields were counted for each assay. Monolayer-inactivated SVECs were wounded by scratching with 1-ml pipette tip. Serum-free medium was added with or without VEGF, bFGF, and CXCL1 (10 ng/ml) and different concentrations of Tpl2 inhibitors. Images were taken by Nikon digital camera after 4 to 8 hours. The migrated cells were quantified by manual counting, and the percentage inhibition was expressed using untreated wells. At least four independent experiments were performed.

*Matrigel Plug Model in Rats (*In Vivo *Angiogenesis)*

Nude mice or C57BL/6 mice were injected subcutaneously with 0.6 ml of Matrigel containing the indicated amount of VEGF or CXCL1 (100 ng/0.6 ml) with or without Tpl2 inhibitor (50 μg/0.6 ml). The injected Matrigel rapidly formed a single, solid gel plug. After 30 days, the skin of the mouse was easily pulled back to expose the Matrigel plug, which remained intact. Hemoglobin was measured using the Drabkin method and a Drabkin reagent kit 525 (Sigma, St Louis, MO) for the quantification of blood vessel formation. Hemoglobin concentration was calculated from a known amount of hemoglobin assayed in parallel. The images were photographed with a Nikon digital camera, and the number of newly formed microvessels was counted.

Immunoprecipitations and Western Blot Analysis

Proteins (80 μg) were separated by sodium dodecyl sulfate–polyacrylamide gel electrophoresis, electrophoretically transferred to nitrocellulose membranes, and blocked for 1 hour in PBS containing Tween 20 (0.1%) and nonfat milk (5%). Blots were incubated with Tpl2, GAPDH, Ki67, and proliferating cell nuclear antigen (PCNA) antibody (Santa Cruz Biotechnology) for 1 hour. Membranes were then incubated for 1 hour with HRP-conjugated secondary antibody. After further washing with PBS, the blots were incubated with commercial chemiluminescence reagents (Amersham Biosciences, Piscataway, NJ). The quantitative analysis of the protein expression was determined by densitometry (Image-Pro Plus software).

VEGF Assay

VEGF concentrations were measured with a human VEGF ELISA kit (R&D Systems, Minneapolis, MN).

Statistical Analysis

Values were presented as means ± SEM. Analysis of variance followed by Fisher least significant difference test were performed for all data. $P < .05$ was considered statistically significant.

Results

Tpl2 Inhibitor Diminished Peritoneal Dissemination

The maximum intensity projection of [^{18}F]-FDG–PET/CT was generated from typical representative mice (Figure 1*A*). Peritoneal

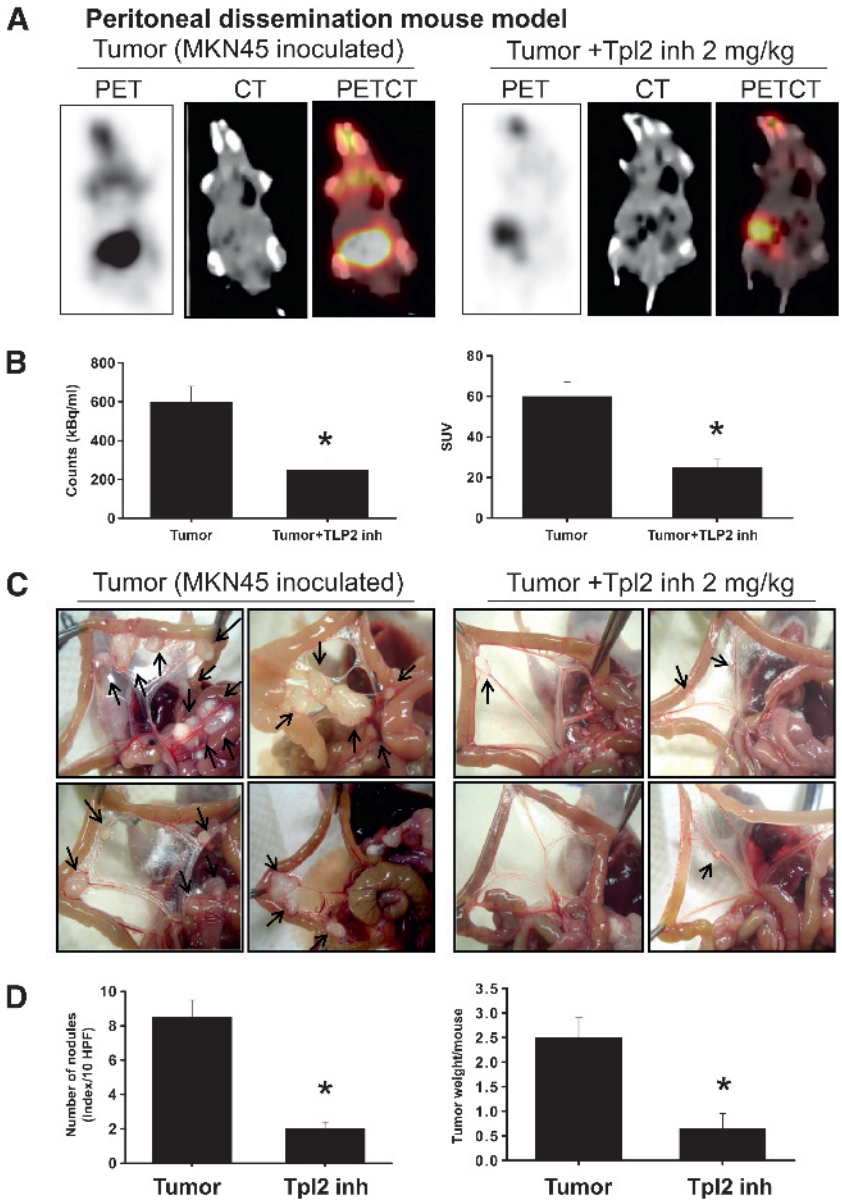

Figure 1. Tpl2 inhibitor diminished peritoneal dissemination. [^{18}F]-FDG–PET served as a representative estimate of therapeutic efficacy. (A) Representative FDG–PET/CT images of animals inoculated with MKN45 gastric cancer cells with or without Tpl2 inhibitor treatment. The maximum intensity projection of typical representative nude mice (left, tumor control; right, Tpl2 inhibitor treatment) showed many metastatic nodules in the mesentery of the control mice inoculated with MKN45 cells. In contrast, peritoneal metastasis was observed sporadically in Tpl2 inhibitor–treated mice. (B) Quantifications of estimated radioactivity (kBq/ml, left panel) and SUVs (right panel) were calculated. SUV was used as an index to determine if a hot spot was significant. (C) Photomacrographs of metastatic peritoneal nodules (arrows shown). (D) Quantifications of nodule number (left panel) and tumor weight (right panel). All data are presented as means ± SEM (n = 6-8). *P < .05 compared to controls.

dissemination was marked in the control mice (left panel), and it was effectively reversed by the Tpl2 inhibitor treatment (right panel). These images demonstrated that noninvasive [^{18}F]-FDG uptake in peritoneal dissemination of control mice was much higher than that in the Tpl2 inhibitor–treated mice. In the quantification of intensity (Figure 1*B*), intraperitoneal injection of Tpl2 inhibitor significantly reduced the estimated radioactivity counts and specific uptake values (SUVs) determined by [^{18}F]-FDG–PET/CT in mice inoculated with gastric cancer cells. Moreover, by macroscopic image capture, the control groups inoculated with MKN45 cells presented with many metastatic nodules in the peritoneal cavity (mesentery; Figure 1*C*). In contrast, peritoneal tumor nodules were observed sporadically in mice treated with Tpl2 inhibitor. The quantification of nodules per field and tumor weight per mice was shown in Figure 1*D*. The results indicated that Tpl2 inhibitor diminished the peritoneal dissemination of gastric tumor cells.

Inhibition of Tpl2 Reduced Tumor Angiogenesis and Prevented HUVEC Proliferation

This study examined microvessel density in tumor in response to Tpl2 inhibitor treatment in tissues using immunohistologic staining of CD31 antibody. Tpl2 inhibitor significantly inhibited tumor angio-

genesis as indicated by reduced MVD in tumor mass (Figure 2*A*). The hypothesis that Tpl2 inhibition could prevent angiogenesis was also tested. Treatment of HUVECs with VEGF, bFGF, or CXCL1 for 24 hours significantly stimulated growth as determined by MTS assay (Figure 2*B*). This increase in growth was attenuated in the presence of Tpl2 inhibitor. In the absence of angiogenic factors, Tpl2 inhibitor alone did not affect the HUVEC growth. To exclude nonspecific effects of a pharmacological inhibitor, the Tpl2 message was ablated by transient transfection of HUVECs with Tpl2 siRNA. Transfection of HUVECs with Tpl2 siRNA, but not scrambled siRNA, caused an 85% ablation of Tpl2 protein (Figure W1). Consistent with previous data, transfection of HUVECs with Tpl2 siRNA significantly inhibited VEGF- and bFGF-induced cell growth by 65% (Figure 2*C*). The inhibitory activity of Tpl2 inhibitor on VEGF-, bFGF-, or CXCL1-induced HUVEC proliferation was also assessed by Western blot analysis using antibody probe with PCNA and Ki67 (data not shown), a proliferation marker. Treatment of HUVECs with VEGF, bFGF, or CXCL1 increased PCNA expression, whereas Tpl2 inhibition

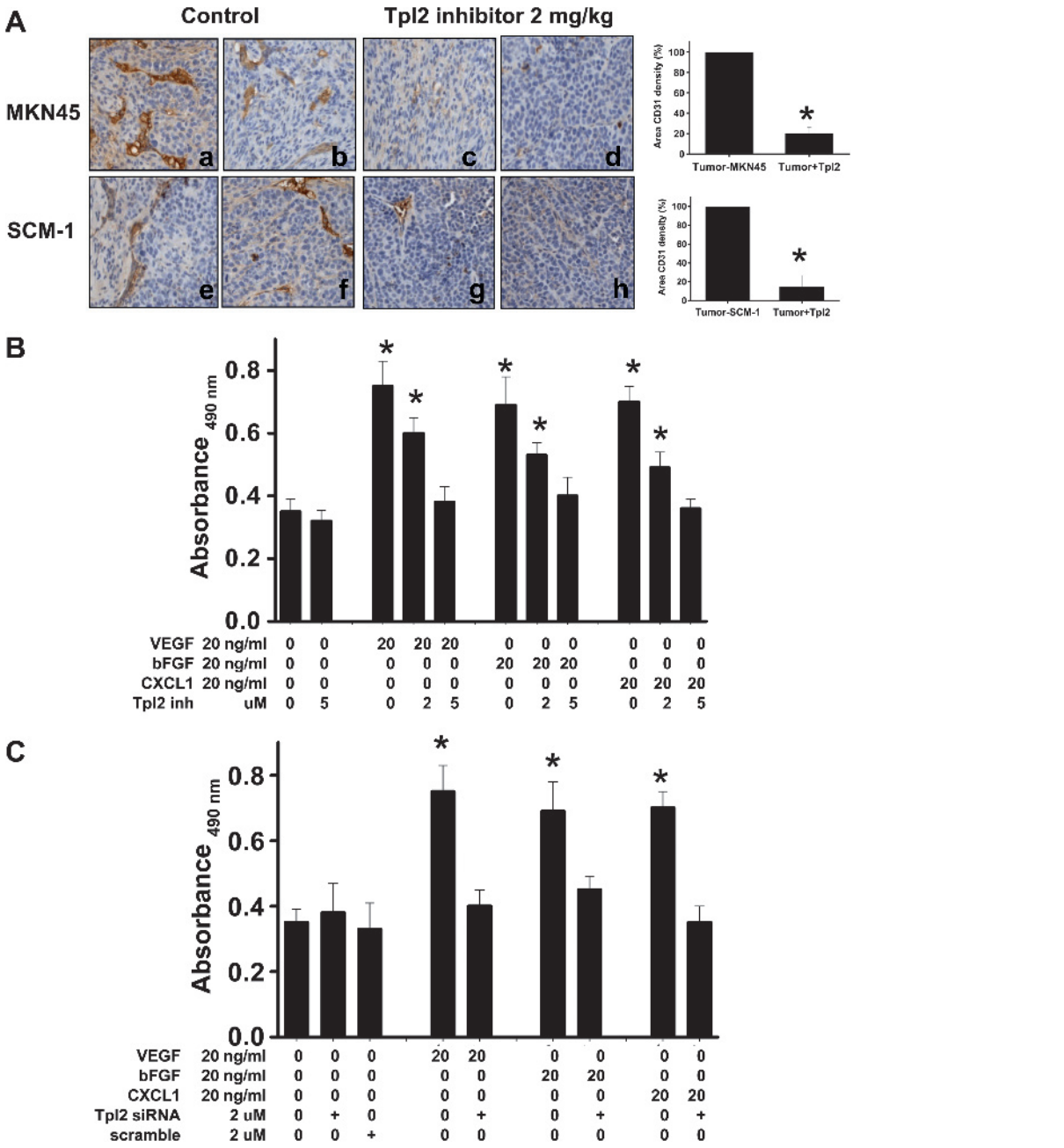

Figure 2. Tpl2 inhibitor reduced tumor angiogenesis and prevented angiogenic factor–induced proliferation of HUVECs. (A) Immunohistochemistry of tumors stained with anti-CD31. Right panel: Quantitation of tumor vasculature indicated that Tpl2 inhibitor prevented angiogenesis. The MVD of CD31 in each section was measured in five images from each treatment ($n = 5$). Bars, MVD in each treatment; original magnification, ×100. (B) HUVECs were preincubated with Tpl2 inhibitor or (C) transfected with Tpl2 siRNA or scrambled Tpl2 siRNA, followed by stimulation with VEGF, bFGF, or CXCL1. Cell viability was determined by MTS assay. All data are presented as means ± SEM of five independent experiments. *$P < .05$ compared to controls.

significantly prevented it. These results suggested that Tpl2 mediated the VEGF-, bFGF-, or CXCL1-induced HUVEC growth.

Angiogenic Factor–Induced Phosphorylation and Activation of Tpl2

To determine whether Tpl2 was involved in cellular response to exposure to pro-angiogenic factors, the expression of Tpl2 induced by pro-angiogenic factors in HUVECs and SVECs was examined. VEGF, bFGF, or CXCL1 exposure caused a substantial elevation of Tpl2 production (Figure 3, *A* and *B*) and kinase activity (Figure 3*C*) in a time-dependent manner and induced the phosphorylation of Tpl2 in a dose-dependent manner (Figure 3*D*). Exposure to bFGF also showed a similar pattern (data not shown). VEGF or CXCL1 induced phosphorylation of Tpl2 in a dose-dependent manner. The level of phosphorylated Tpl2 or total Tpl2 protein was determined by Western blot analysis. The relative value of density for phosphorylation of Tpl2 bands was normalized to Tpl2, and this was consistent with kinase activity of Tpl2 (data not shown). These results indicated that VEGF or CXCL1 induced protein expression, as well as the phosphorylation and kinase activity of Tpl2 in endothelial cells.

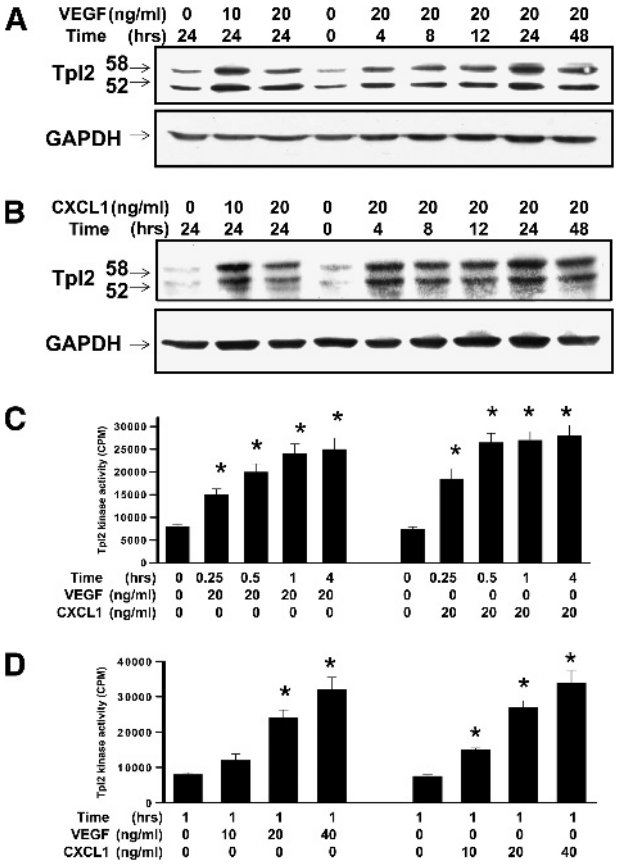

Figure 3. Angiogenic factor–induced phosphorylation and activation of Tpl2. VEGF or CXCL1 induced the phosphorylation of Tpl2 in a time- and dose-dependent manner. (A) Cells were exposed to VEGF or (B) CXCL1 and harvested at the indicated time. Levels of Tpl2 or GAPDH proteins were determined by Western blot analysis at the indicated concentration. (C) VEGF or CXCL1 induced Tpl2 kinase activity in a time-course response. (D) VEGF or CXCL1 induced Tpl2 kinase activity in a dose-dependent manner. Cells were disrupted and kinase activity of Tpl2 was determined as described in the Materials and Methods section. All data are presented as means ± SEM of five independent experiments. $^*P < .05$ compared to controls.

Inhibition of Tpl2 Prevented Endothelial Cell Tube Formation In Vitro

The effect of Tpl2 inhibition on tube formation induced by angiogenic factors in HUVECs was examined. Inhibition by Tpl2 inhibitor prevented angiogenic factors like VEGF-, bFGF-, and CXCL1-induced (Figure 4, *A–C*) endothelial cell tube formation in a concentration-dependent manner. The endothelial cell tube formation by HUVECs was completely abolished at a higher concentration (5 μM) of Tpl2 inhibitor. Consistent with data obtained with the Tpl2 inhibitor, transfection of HUVECs with Tpl2-siRNA significantly inhibited VEGF-, bFGF-, and CXCL1-induced tube formation by 75% (Figure W2). Scrambled RNA *per se* did not have any effect. These results demonstrated that Tpl2 inhibition prevented VEGF-, bFGF-, and CXCL1-induced angiogenesis in HUVECs.

Inhibition of Tpl2 Prevented Angiogenic Factor–Induced Angiogenesis In Vivo

To determine whether Tpl2 inhibitor is capable of blocking VEGF-induced angiogenesis *in vivo*, an established *in vivo* angiogenesis model, the mouse Matrigel plug assay, was performed. Plugs with VEGF or CXCL1 alone were markedly streaky, vascular, and red. Plugs with Matrigel alone and containing VEGF and Tpl2 inhibitor or CXCL1 and Tpl2 inhibitor were pallid, indicating less blood vessel formation (Figure 4, *D* and *E*). Vessel density and vessel morphology in the plug sections were also examined by H&E staining and immunohistochemical staining with an antibody against CD31, an endothelial cell marker. Vascularization in the Tpl2 inhibitor plus VEGF or CXCL1 group was significantly reduced compared to that in the VEGF alone group (Figure 4*F*). Quantification of the vascularization by counting the vessels (Figure 4*G*) and endothelial cells (Figure 4*H*) revealed that the vascular density in the Tpl2 inhibitor–treated group was significantly decreased. These indicated that the Tpl2 inhibitor was capable of inhibiting VEGF- or CXCL1-induced neovessel formation *in vivo*.

Inhibition of Tpl2 Prevented Angiogenic Factor–Induced Vessel Sprouting in an Aortic Ring Assay Ex Vitro

The sprouting of vessels from aortic rings was investigated to determine whether Tpl2 inhibitor blocked VEGF-induced angiogenesis *ex vivo*. Extensive endothelial cell outgrowth from rat aorta ring explants was observed in the control group (Figure 5*A*). Tpl2 inhibitor treatment resulted in a significant (about six-fold) reduction of endothelial outgrowth and sprouting from aortic rings (Figure 5*B*), suggesting that Tpl2 inhibition resulted in a significant reduction in VEGF-induced vessel sprouting in a dose-dependent manner.

Inhibition of Tpl2 Prevented Angiogenic Factor–Induced Chemotactic Motility and Migration of HUVECs and SVECs

The effects of Tpl2 inhibition on chemotactic motility of HUVECs and SVECs were measured using either Transwell chamber assay or wound scratch model assay. Tpl2 inhibition prevented the VEGF-induced chemotactic motility of both HUVECs and SVECs in a concentration-dependent manner (Figure 5, *C* and *D*). However, Tpl2 inhibition alone had no significant effect on basal migration of endothelial cells. The effect of Tpl2 inhibition on VEGF-induced

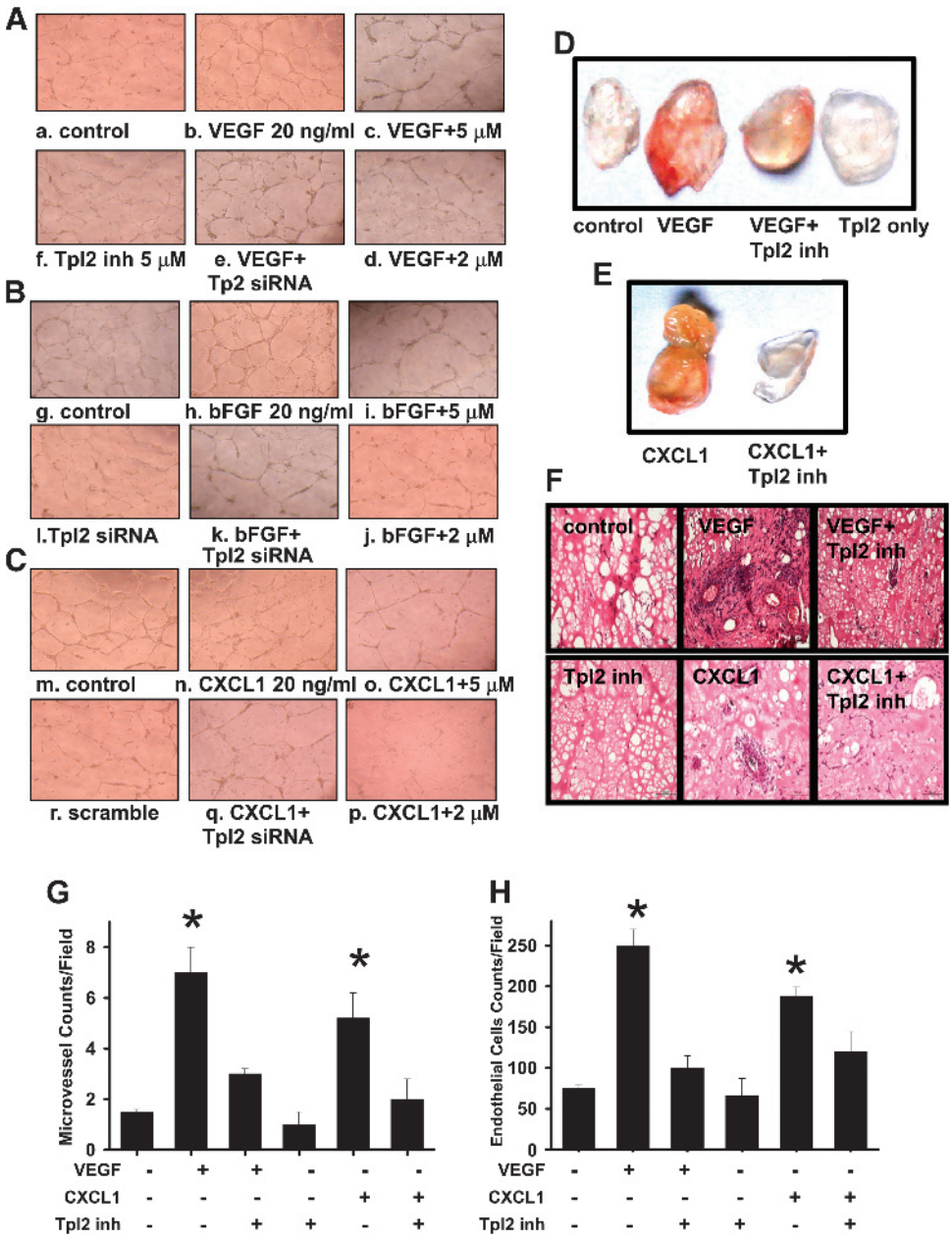

Figure 4. Inhibition of Tpl2 prevented angiogenic factor–induced endothelial cell tube formation *in vitro* and *in vivo* Matrigel plug assay. Tpl2 inhibitor or Tpl2 siRNA suppressed the endothelial cell tube formation. HUVECs preincubated with Tpl2 inhibitor or transfected with Tpl2 siRNA or scrambled Tpl2 siRNA were stimulated with (A) VEGF, (B) bFGF, or (C) CXCL1. Tube formation images were captured in an inverted photomicroscope (left panel), and tube formations were scored. For the *in vivo* Matrigel plug assay, (D) and (E) represented Matrigel plugs and (F) represented H&E staining of sections from Matrigel plugs. (G) Quantifications of vessel numbers and (H) endothelial cells in Matrigel plug sections (counts/field) were calculated. The numbers in each case were the average of five different slides and five regions per slide. All data are presented as means ± SEM of three independent experiments ($n = 3$). *$P < .05$ compared to controls.

migration of HUVECs and SVECs was determined using the wound scratch model assay (Figure 5, *E* and *F*). Inhibition of Tpl2 by pharmacological inhibitor or ablation of Tpl2 using specific siRNA significantly prevented endothelial cell migration. Thus, Tpl2 inhibition prevented the invasion and migration of endothelial cells.

Constraint of Tpl2 Blocks C/EBPβ, NF-κB, and AP1 Activation

The *VEGF* gene contained C/EBPβ, NF-κB, and AP1 binding sites within its promoter, thereby activating transcription and gene expression. To determine the transcriptional activity and VEGF expression of endothelial cells in response to CXCL1 and EGF, the expression of transcriptional activity was measured by luciferase reporter assay. Cells pretreated with Tpl2 inhibitor markedly inhibited CXCL1- or EGF-induced C/EBPβ, NF-κB, and AP1 activation. A Tpl2 siRNA was transfected into SVECs, which were then transfected with a C/EBPβ, NF-κB, and AP1 luciferase plasmid. CXCL1 or EGF treatment decreased C/EBPβ, NF-κB, and AP1-dependent transcriptional activity in Tpl2 siRNA cells compared to control scrambled RNA cells (Figure 6, *A*–*C*). These data showed that

C/EBPβ, NF-κB, and AP1 were downstream regulators of Tpl2 for CXCL1- or EGF-induced VEGF expression. In addition, transfection of Tpl2 siRNA into cells also inhibited the generation of VEGF (Figure 6*D*). The combination of Tpl2 inhibitor with CXCL1 or EGF in cells also markedly reduced VEGF production when compared to either treatment alone. These results indicated that Tpl2 was a potent anti-angiogenic molecule.

Discussion

A major form of tumor recurrence is peritoneal dissemination, and a crucial problem in such tumor growths is tumor angiogenesis [38–41]. Angiogenesis plays a critical role in the fundamental physiologic process and pathologic neovascularization. Solid tumors in the early stage secrete VEGF and other pro-angiogenic factors to evoke tumor angiogenesis [42,43]. The main signaling circuit of VEGF is thought to

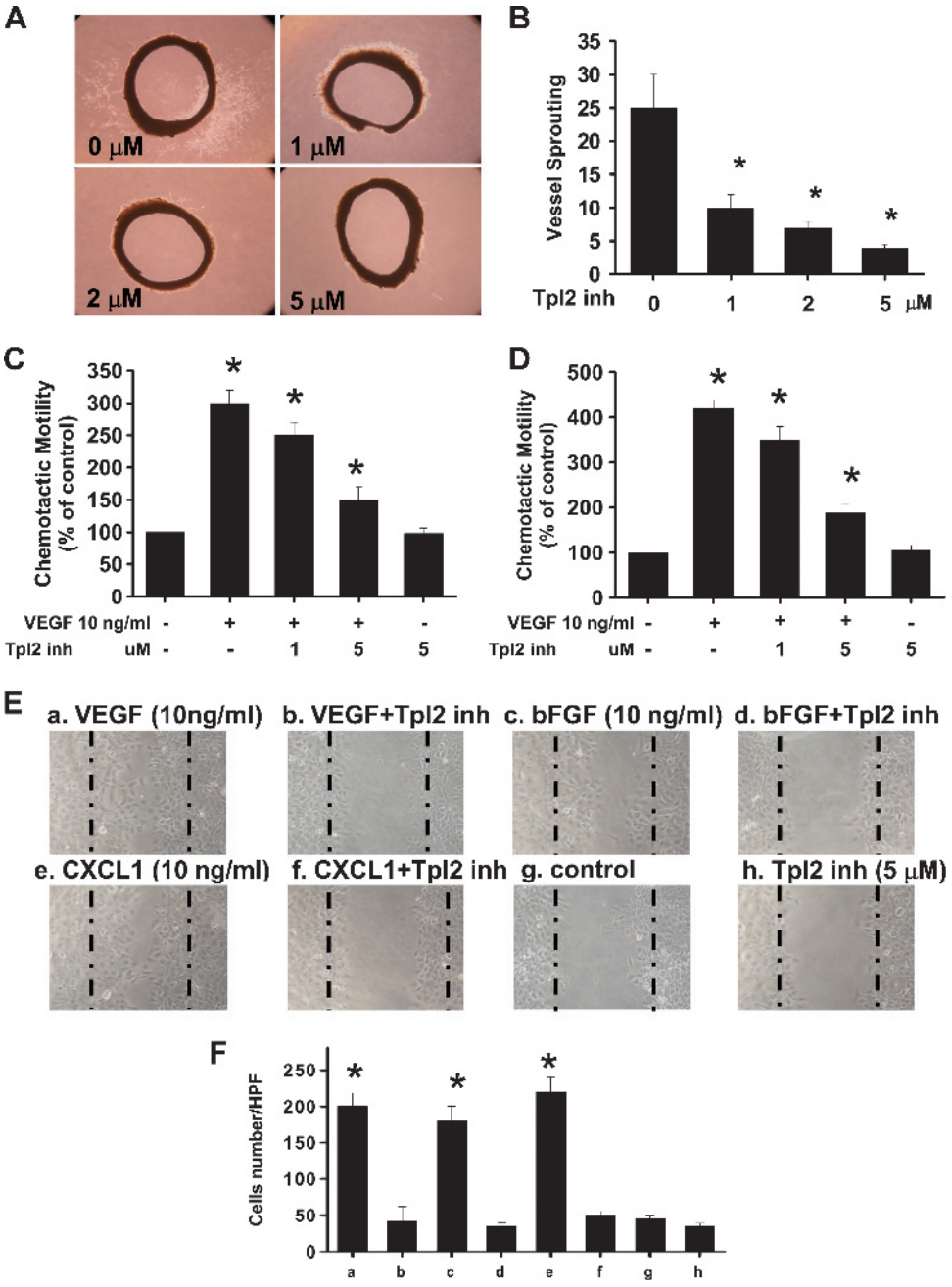

Figure 5. Inhibition of Tpl2 prevented angiogenic factor–induced vessel sprouting in an aortic ring assay *ex vitro*, chemotactic motility, and migration of HUVECs and SVECs. (A) Tpl2 inhibitor inhibited endothelial cell sprouting in an aortic ring assay. (B) The endothelial cell sprouting was abundant in the control aortic rings but not in the rings treated with Tpl2 inhibitor. (C) HUVECs or (D) SVECs were pretreated with various concentrations of Tpl2 inhibitor before VEGF treatment. After incubation, chemotaxis was quantified by counting the cells that migrated to the lower side of the filter with optical microscopy at ×200 magnification. The basal migration in the absence of VEGF was 100 ± 10 cells/field. (E) Tpl2 inhibitor inhibited SVEC migration. Cells migrating into the wound area were counted on the basis of the dash line. The representative photographs showed the same area at 12 hours with VEGF, bFGF, and CXCL1 and before preincubation with or without Tpl2 inhibitor. (F) These results were representative of four independent experiments. *$P < .05$ compared to controls.

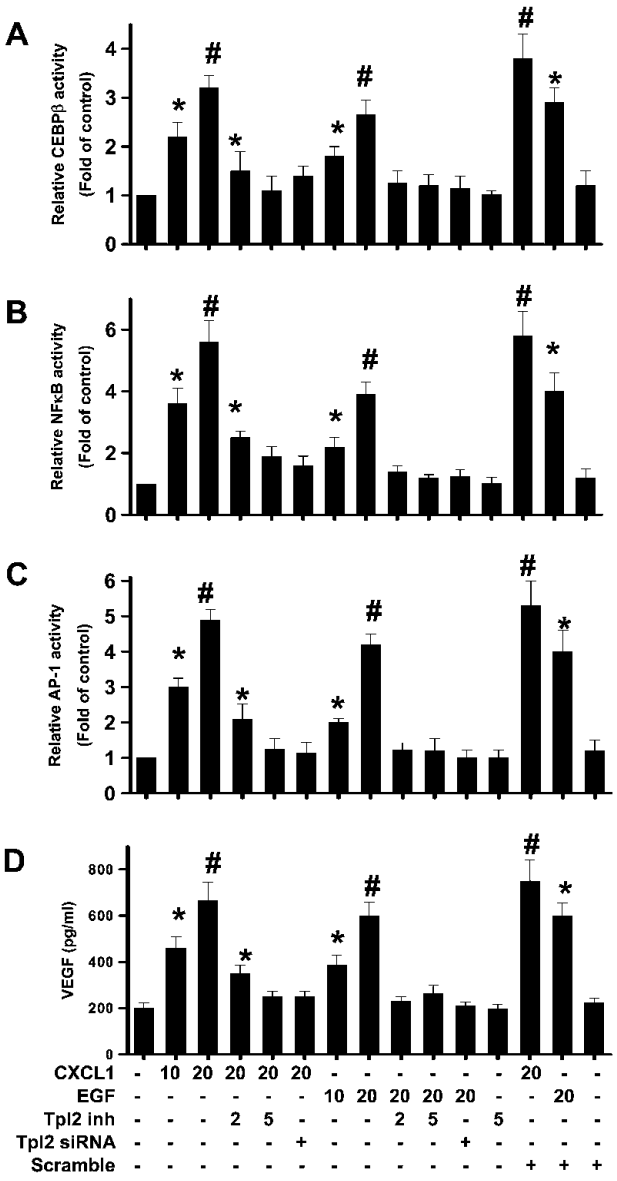

Figure 6. Constraint of Tpl2 blocked C/EBPβ, NF-κB, and AP1 activation. Tpl2 inhibitor or Tpl2 siRNA inhibited VEGF-, bFGF-, and CXCL1-induced C/EBPβ, NF-κB, and AP1 promoter activity. Endothelial cells (SVECs) that were transiently transfected with the (A) C/EBPβ, (B) NF-κB, and (C) AP1 luciferase reporter plasmid and a thymidine kinase promoter–driven Renilla-luciferase vector were transiently transfected with Tpl2 siRNA or control scrambled RNA and treated with VEGF, bFGF, and CXCL1. The relative activity was measured by luciferase assay as described in the Materials and Methods section. Means ± SEM of luciferase activities were calculated from triplicate determinations. (D) Tpl2 inhibitor or Tpl2 siRNA reduced VEGF-, bFGF-, and CXCL1-induced VEGF secretion. VEGF generation was determined using the VEGF ELISA kit as described in the Materials and Methods section. All data were presented in four determinations. *$P < .01$, for significant difference between groups.

involve activation of transcription factors, which are implicated in all critical endothelial functions, including proliferation, migration, and angiogenesis. Other potent pro-angiogenic factors like EGF, bFGF, and CXCL1 evoke vast amount of transcription factors that can trigger a signaling pathway involved in the growth of endothelial cells [44–46]. The results suggest that Tpl2 is upstream of the transcription factors. More importantly, the findings here reveal for the first time that Tpl2-mediated angiogenesis is characteristic of endothelial cells *in vitro*, *in vivo*, and *ex vivo*, indicating a novel anti-angiogenic function of Tpl2 inhibitors that control transcription factors.

Many transcription factors have been shown to regulate VEGF in response to angiogenesis, including NF-κB, C/EBPβ, AP1, SP-1, STAT-3, and HIF-1α [18,27,31,47]. However, although factors relay available pro-angiogenic factors to functional endothelial cells, none of them accounts for the actual targeting of Tpl2. Proto-oncogene Tpl2 is a serine-threonine kinase that integrates signals from Toll receptors, cytokine receptors, progression of rodent T cell lymphomas, and T cell activation [5,48,49]. Overexpression of Tpl2 has been found in breast cancer, gastric cancer, and colon adenocarcinoma [6–8]. Paradoxically, loss of Tpl2 enhances tumorigenesis and inflammation in two-stage skin carcinogenesis, indicating that Tpl2 may serve more as a tumor suppressor than as an oncogene in chemically induced skin carcinogenesis, its absence contributing to both tumorigenesis and inflammation [50]. Interestingly, Tpl2 ablation promotes intestinal inflammation and tumorigenesis in Apc^{min} mice by inhibiting interleukin-10 secretion and regulatory T cell generation, suggesting that Tpl2 also has a critical role in regulating systemic inflammation and in the susceptibility to intestinal tumorigenesis [51]. Tpl2 knockout mice are resistant to lipopolysaccharide (LPS)/D-galactosamine–induced pathology, because of the low production of tumor necrosis factor–α among other cytokines, implying that endogenous Tpl2 may be involved in innate and adaptive immunity rather in proliferative signals physiologically [52]. Although previous studies suggest that Tpl2 possesses different functions, the role of Tpl2 in endothelial cells and in regulating angiogenesis remains poorly understood. The present study shows that Tpl2 inhibitor markedly diminishes tumor peritoneal dissemination and reduces tumor angiogenesis in a mouse model. Other evidence demonstrates that Tpl2 inhibitor causes tumor burden changes and inhibits tumor growth within 2 weeks. These changes are consistent with the results of PET/CT imaging studies and nodule counts in the present study. Therefore, constitutively high levels of Tpl2 activity may disturb cell regulation and lead to abnormal functioning in cells.

Previous reports have shown that transcription factors are overactive in most human cancer cells and are thus suitable potential targets for the development of anticancer drugs. Darnell et al. reported that to be considered an ideal target for cancer therapy, a transcription factor needs to fulfill four main criteria [24]. However, in spite of an ever-increasing number of putative small molecule inhibitors of transcription factors, only a handful are currently progressing through preclinical and early clinical development. Cytoplasmic proteins activate transcription factors further, then relay the signal into the nucleus and change the transcription pattern of the cell, with the ultimate outcome of upregulating or downregulating gene expression. Thus, targeted disruption of Tpl2 in the endothelial cell growth to decrease angiogenesis and peritoneal dissemination is a promising strategy. Tpl2 is reported to be capable of activating both the mitogen-activated protein kinase and c-jun-N-terminal kinase (JNK) kinase pathways. In addition, the Tpl2 kinase can activate transcription factors such as inhibitor of NFκB (IκB) kinases and can induce the nuclear production of NF-κB [53]. Li et al. have shown that the Tpl2/AP1 signaling transduction pathway is a positive regulator of MHV-68 lytic replication [54]. However, in the present study, an inhibitor of Tpl2 comprehensively blocks C/EBPβ, NF-κB, and AP1 activation in pro-angiogenic factor–induced activation

of endothelial cells. Simultaneously, Tpl2 inhibition can block cancer cell survival, proliferation, and tumor growth reduction in an animal study (data not shown). These findings suggest that regulating the function of Tpl2 and the subsequent control of transcription factor activity may provide a new therapeutic strategy against pathologic diseases. Moreover, circulating VEGF seems to be a reliable surrogate marker of angiogenic activity and tumor progression in cancer patients. On the basis of these observations, targeting the VEGF signaling cascade may be a useful component of an anti-angiogenic strategy. The results here demonstrate that the addition of Tpl2 inhibitors significantly reduces CXCL1- or bFGF-induced VEGF production, which may provide insights into potential strategies for preventing the development of angiogenesis and metastasis. This also opens a potential role of anti-angiogenic therapy in suppressing the development of metastases after cancer resection. The candidate gene *Tpl2* appears to exhibit the most direct action and may therefore have the potential as a target for cancer treatment.

Vascular endothelial cells respond to alarm signals of the body by angiogenesis or inflammation [55]. Inflammatory tissue is often hypoxic, which can induce angiogenesis through the up-regulation of factors such as VEGF [56]. Moreover, a previous report shows that VEGF-A induces the recruitment of leukocytes to the inflamed intestine *in vivo*, thus fostering inflammation. These strongly support the important role played by the VEGF pathway in both inflammation and angiogenesis underlying disease pathogenesis in inflammatory bowel disease (IBD) [57]. There is considerable evidence to suggest that angiogenesis and chronic inflammation are co-dependent. Conversely, inhibition of angiogenesis is predicted to diminish chronic inflammatory responses and several examples of this have been observed [56,58]. In the present work, angiogenic factors VEGF, CXCL1, and bFGF have markedly induced Tpl2 activation and endothelial cell proliferation. Tpl2 inhibitors effectively reverse angiogenesis in activated endothelial cells. Thus, it can be considered that Tpl2 inhibitors, specifically inhibitors of angiogenesis, are new targets, and the intriguing connection between angiogenesis and inflammation can be further explored. Pharmacologic control of angiogenesis may hold great promise for the alleviation of inflammatory states.

Angiogenesis and lymphogenesis are commonly seen in tumor masses, especially at the tumor margins. Detection of MVD and lymphatic vessel density (LVD) at tumor borders may be useful in predicting metastasis and in prognosticating in patients with a tumor mass. In particular, co-accounting of MVD and LVD may be a useful prognostic factor in tumor masses. Lymphatic endothelial cell marker hyaluronan receptor LYVE-1 and CD31, also known as platelet endothelial cell adhesion molecule 1, are used primarily to demonstrate the presence of endothelial cells in histologic tissue sections [59–62]. These markers can help evaluate the degree of extension and growth of tumor endothelial cells, which can indicate a rapidly growing tumor. Malignant endothelial cells also commonly retain the antigens, so CD31 and LYVE-1. Immunohistochemistry may be used to demonstrate their presence. In addition, the aforementioned finding has been proven in animal models and clinicopathologic studies [59–62]. Emerging evidence show that vascular targeting agents are aimed specifically at the existing tumor vasculature. Anti-angiogenic agents target angiogenesis or the new growth of tumor vessels. The present study uses primary HUVECs, which are cells derived from the endothelium of veins from the umbilical cord, for angiogenesis. Moreover, mouse lymphoid microvascular endothelial immortalized cell line (SVEC) can indicate the probable therapeutic efficacy in lymphogenesis. The inhibition of Tpl2 can prevent *in vivo*, *in vitro*, and *ex vivo* angiogenesis in a mouse model. Angiogenesis and lymphogenesis, which are dependent on endothelial cells, are important in the growth and metastasis of solid tumors and are regulated by Tpl2 activation. For the first time, the present study shows that Tpl2 is an excellent novel therapeutic target for the prevention of angiogenesis and suggests that it may be a highly promising stratagem for lymphogenesis therapy in the future.

In conclusion, the inhibition of Tpl2 prevents angiogenesis *in vivo*, *in vitro*, and *ex vivo*. Tpl2 inhibition diminishes peritoneal dissemination and tumor angiogenesis. The Tpl2-mediated inhibition of peritoneal endothelial cell growth, chemotactic motility, and migration is associated with blockade of pro-angiogenic growth factor–induced transcription factor activity and the down-regulation of VEGF expression. There is a novel role of Tpl2 in regulating the angiogenic process and inhibiting it may prevent cancer growth and peritoneal dissemination by ameliorating angiogenesis. Hence, Tpl2 inhibitors can lead to the development of pharmaceutical drugs for the treatment of angiogenesis-dependent human diseases like tumors.

Acknowledgments

The authors thank the Department of Education and Research of Taichung Veterans General Hospital and Gene Alzona Nisperos for their excellent assistance with the editing of this manuscript.

References

[1] Risco A, del Fresno FC, Mambol A, Alsina-Beauchamp D, MacKenzie KF, Yang HT, Barber DF, Morcelle C, Arthur JS, Ley SC, et al. (2012). p38γ and p38δ kinases regulate the Toll-like receptor 4 (TLR4)-induced cytokine production by controlling ERK1/2 protein kinase pathway activation. *Proc Natl Acad Sci USA* **109**, 11200–11205.

[2] Mielke LA, Elkins KL, Wei L, Starr R, Tsichlis PN, O'Shea JJ, and Watford WT (2009). Tumor progression locus 2 (Map3k8) is critical for host defense against *Listeria monocytogenes* and IL-1β production. *J Immunol* **183**, 7984–7993.

[3] Cho J, Melnick M, Solidakis GP, and Tsichlis PN (2005). Tpl2 (tumor progression locus 2) phosphorylation at Thr^{290} is induced by lipopolysaccharide via an Iκ-B kinase-β-dependent pathway and is required for Tpl2 activation by external signals. *J Biol Chem* **280**, 20442–20448.

[4] Watford WT, Wang CC, Tsatsanis C, Mielke LA, Eliopoulos AG, Daskalakis C, Charles N, Odom S, Rivera J, O'Shea J, et al. (2010). Ablation of tumor progression locus 2 promotes a type 2 Th cell response in ovalbumin-immunized mice. *J Immunol* **184**, 105–113.

[5] Christoforidou AV, Papadaki HA, Margioris AN, Eliopoulos GD, and Tsatsanis C (2004). Expression of the Tpl2/Cot oncogene in human T-cell neoplasias. *Mol Cancer* **3**, 34.

[6] Krcova Z, Ehrmann J, Krejci V, Eliopoulos A, and Kolar Z (2008). Tpl-2/Cot and COX-2 in breast cancer. *Biomed Pap Med Fac Univ Palacky Olomouc Czech Repub* **152**, 21–25.

[7] Sourvinos G, Tsatsanis C, and Spandidos DA (1999). Overexpression of the Tpl-2/Cot oncogene in human breast cancer. *Oncogene* **18**, 4968–4973.

[8] Ohara R, Hirota S, Onoue H, Nomura S, Kitamura Y, and Toyoshima K (1995). Identification of the cells expressing cot proto-oncogene mRNA. *J Cell Sci* **108**(Pt 1), 97–103.

[9] Hatziapostolou M, Polytarchou C, Panutsopulos D, Covic L, and Tsichlis PN (2008). Proteinase-activated receptor-1–triggered activation of tumor progression locus-2 promotes actin cytoskeleton reorganization and cell migration. *Cancer Res* **68**, 1851–1861.

[10] Jeong JH, Bhatia A, Toth Z, Oh S, Inn KS, Liao CP, Roy-Burman P, Melamed J, Coetzee GA, and Jung JU (2011). *TPL2/COT/MAP3K8* (*TPL2*) activation promotes androgen depletion-independent (ADI) prostate cancer growth. *PLoS One* **6**, e16205.

[11] Lee KM, Lee KW, Bode AM, Lee HJ, and Dong Z (2009). Tpl2 is a key mediator of arsenite-induced signal transduction. *Cancer Res* **69**, 8043–8049.

[12] Brower V (2009). How well do angiogenesis inhibitors work? Biomarkers of response prove elusive. *J Natl Cancer Inst* **101**, 846–847.
[13] Hussain S, Slevin M, Matou S, Ahmed N, Choudhary MI, Ranjit R, West D, and Gaffney J (2008). Anti-angiogenic activity of sesterterpenes; natural product inhibitors of FGF-2-induced angiogenesis. *Angiogenesis* **11**, 245–256.
[14] Cao R, Ji H, Feng N, Zhang Y, Yang X, Andersson P, Sun Y, Tritsaris K, Hansen AJ, Dissing S, et al. (2012). Collaborative interplay between FGF-2 and VEGF-C promotes lymphangiogenesis and metastasis. *Proc Natl Acad Sci USA* **109**, 15894–15899.
[15] Komuro A, Yashiro M, Iwata C, Morishita Y, Johansson E, Matsumoto Y, Watanabe A, Aburatani H, Miyoshi H, Kiyono K, et al. (2009). Diffuse-type gastric carcinoma: progression, angiogenesis, and transforming growth factor β signaling. *J Natl Cancer Inst* **101**, 592–604.
[16] Warner KA, Miyazawa M, Cordeiro MM, Love WJ, Pinsky MS, Neiva KG, Spalding AC, and Nor JE (2008). Endothelial cells enhance tumor cell invasion through a crosstalk mediated by CXC chemokine signaling. *Neoplasia* **10**, 131–139.
[17] Tan DS, Agarwal R, and Kaye SB (2006). Mechanisms of transcoelomic metastasis in ovarian cancer. *Lancet Oncol* **7**, 925–934.
[18] Liu SH, Wang KB, Lan KH, Lee WJ, Pan HC, Wu SM, Peng YC, Chen YC, Shen CC, Cheng HC, et al. (2012). Calpain/SHP-1 interaction by Honokiol dampening peritoneal dissemination of gastric cancer in *nu/nu* mice. *PLoS One* **7**, e43711.
[19] Malz M, Weber A, Singer S, Riehmer V, Bissinger M, Riener MO, Longerich T, Soll C, Vogel A, Angel P, et al. (2009). Overexpression of far upstream element binding proteins: a mechanism regulating proliferation and migration in liver cancer cells. *Hepatology* **50**, 1130–1139.
[20] Schulz P, Fischer C, Detjen KM, Rieke S, Hilfenhaus G, von MZ, Bohmig M, Koch I, Kehrberger J, Hauff P, et al. (2011). Angiopoietin-2 drives lymphatic metastasis of pancreatic cancer. *FASEB J* **25**, 3325–3335.
[21] Akino T, Hida K, Hida Y, Tsuchiya K, Freedman D, Muraki C, Ohga N, Matsuda K, Akiyama K, Harabayashi T, et al. (2009). Cytogenetic abnormalities of tumor-associated endothelial cells in human malignant tumors. *Am J Pathol* **175**, 2657–2667.
[22] Hida K, Hida Y, Amin DN, Flint AF, Panigrahy D, Morton CC, and Klagsbrun M (2004). Tumor-associated endothelial cells with cytogenetic abnormalities. *Cancer Res* **64**, 8249–8255.
[23] Tchaicha JH, Mobley AK, Hossain MG, Aldape KD, and McCarty JH (2010). A mosaic mouse model of astrocytoma identifies αvβ8 integrin as a negative regulator of tumor angiogenesis. *Oncogene* **29**, 4460–4472.
[24] Darnell JE Jr. (2002). Transcription factors as targets for cancer therapy. *Nat Rev Cancer* **2**, 740–749.
[25] Niu J, Chang Z, Peng B, Xia Q, Lu W, Huang P, Tsao MS, and Chiao PJ (2007). Keratinocyte growth factor/fibroblast growth factor-7-regulated cell migration and invasion through activation of NF-κB transcription factors. *J Biol Chem* **282**, 6001–6011.
[26] Royds JA, Dower SK, Qwarnstrom EE, and Lewis CE (1998). Response of tumour cells to hypoxia: role of p53 and NFkB. *Mol Pathol* **51**, 55–61.
[27] Watari K, Nakamura M, Fukunaga Y, Furuno A, Shibata T, Kawahara A, Hosoi F, Kuwano T, Kuwano M, and Ono M (2012). The antitumor effect of a novel angiogenesis inhibitor (an octahydronaphthalene derivative) targeting both VEGF receptor and NF-κB pathway. *Int J Cancer* **131**, 310–321.
[28] Chun KS, Kundu JK, Park KK, Chung WY, and Surh YJ (2006). Inhibition of phorbol ester-induced mouse skin tumor promotion and COX-2 expression by celecoxib: C/EBP as a potential molecular target. *Cancer Res Treat* **38**, 152–158.
[29] Kagan BL, Henke RT, Cabal-Manzano R, Stoica GE, Nguyen Q, Wellstein A, and Riegel AT (2003). Complex regulation of the fibroblast growth factor-binding protein in MDA-MB-468 breast cancer cells by CCAAT/enhancer-binding protein β. *Cancer Res* **63**, 1696–1705.
[30] Su JL, Yang PC, Shih JY, Yang CY, Wei LH, Hsieh CY, Chou CH, Jeng YM, Wang MY, Chang KJ, et al. (2006). The VEGF-C/Flt-4 axis promotes invasion and metastasis of cancer cells. *Cancer Cell* **9**, 209–223.
[31] Wood LD, Farmer AA, and Richmond A (1995). HMGI(Y) and Sp1 in addition to NF-κB regulate transcription of the MGSA/GRO α gene. *Nucleic Acids Res* **23**, 4210–4219.
[32] Luan J, Shattuck-Brandt R, Haghnegahdar H, Owen JD, Strieter R, Burdick M, Nirodi C, Beauchamp D, Johnson KN, and Richmond A (1997). Mechanism and biological significance of constitutive expression of MGSA/GRO chemokines in malignant melanoma tumor progression. *J Leukoc Biol* **62**, 588–597.
[33] Amiri KI, Ha HC, Smulson ME, and Richmond A (2006). Differential regulation of CXC ligand 1 transcription in melanoma cell lines by poly(ADP-ribose) polymerase-1. *Oncogene* **25**, 7714–7722.
[34] Nirodi C, NagDas S, Gygi SP, Olson G, Aebersold R, and Richmond A (2001). A role for poly(ADP-ribose) polymerase in the transcriptional regulation of the melanoma growth stimulatory activity (*CXCL1*) gene expression. *J Biol Chem* **276**, 9366–9374.
[35] Yang J, McNeish B, Butterfield C, and Moses MA (2012). Lipocalin 2 is a novel regulator of angiogenesis in human breast cancer. *FASEB J* **27**, 45–50.
[36] Liu SH, Sheu WH, Lee MR, Lee WJ, Yi YC, Yang TJ, Jen JF, Pan HC, Shen CC, Chen WB, et al. (2012). Advanced glycation end product N^{ε}-carboxymethyllysine induces endothelial cell injury: the involvement of SHP-1-regulated VEGFR-2 dephosphorylation. *J Pathol* **230**, 215–227.
[37] Liu SH, Yang CN, Pan HC, Sung YJ, Liao KK, Chen WB, Lin WZ, and Sheu ML (2010). IL-13 downregulates PPAR-γ/heme oxygenase-1 via ER stress-stimulated calpain activation: aggravation of activated microglia death. *Cell Mol Life Sci* **67**, 1465–1476.
[38] Aoyagi K, Kouhuji K, Yano S, Miyagi M, Imaizumi T, Takeda J, and Shirouzu K (2005). VEGF significance in peritoneal recurrence from gastric cancer. *Gastric Cancer* **8**, 155–163.
[39] Liu Y, Han ZP, Zhang SS, Jing YY, Bu XX, Wang CY, Sun K, Jiang GC, Zhao X, Li R, et al. (2011). Effects of inflammatory factors on mesenchymal stem cells and their role in the promotion of tumor angiogenesis in colon cancer. *J Biol Chem* **286**, 25007–25015.
[40] Klauber-Demore N (2012). Are epsins a therapeutic target for tumor angiogenesis? *J Clin Invest* **122**, 4341–4343.
[41] Kerbel RS (2000). Tumor angiogenesis: past, present and the near future. *Carcinogenesis* **21**, 505–515.
[42] Ribatti D (2011). Novel angiogenesis inhibitors: addressing the issue of redundancy in the angiogenic signaling pathway. *Cancer Treat Rev* **37**, 344–352.
[43] Butler JM, Kobayashi H, and Rafii S (2010). Instructive role of the vascular niche in promoting tumour growth and tissue repair by angiocrine factors. *Nat Rev Cancer* **10**, 138–146.
[44] Bonavia R, Inda MM, Vandenberg S, Cheng SY, Nagane M, Hadwiger P, Tan P, Sah DW, Cavenee WK, and Furnari FB (2012). EGFRvIII promotes glioma angiogenesis and growth through the NF-κB, interleukin-8 pathway. *Oncogene* **31**, 4054–4066.
[45] Bobrovnikova-Marjon EV, Marjon PL, Barbash O, Vander Jagt DL, and Abcouwer SF (2004). Expression of angiogenic factors vascular endothelial growth factor and interleukin-8/CXCL8 is highly responsive to ambient glutamine availability: role of nuclear factor-κB and activating protein-1. *Cancer Res* **64**, 4858–4869.
[46] Kishimoto K, Liu S, Tsuji T, Olson KA, and Hu GF (2005). Endogenous angiogenin in endothelial cells is a general requirement for cell proliferation and angiogenesis. *Oncogene* **24**, 445–456.
[47] Dong W, Li Y, Gao M, Hu M, Li X, Mai S, Guo N, Yuan S, and Song L (2012). IKKα contributes to UVB-induced VEGF expression by regulating AP-1 transactivation. *Nucleic Acids Res* **40**, 2940–2955.
[48] Hirata K, Taki H, Shinoda K, Hounoki H, Miyahara T, Tobe K, Ogawa H, Mori H, and Sugiyama E (2010). Inhibition of tumor progression locus 2 protein kinase suppresses receptor activator of nuclear factor-κB ligand-induced osteoclastogenesis through down-regulation of the c-Fos and nuclear factor of activated T cells c1 genes. *Biol Pharm Bull* **33**, 133–137.
[49] Watford WT, Hissong BD, Durant LR, Yamane H, Muul LM, Kanno Y, Tato CM, Ramos HL, Berger AE, Mielke L, et al. (2008). Tpl2 kinase regulates T cell interferon-γ production and host resistance to *Toxoplasma gondii*. *J Exp Med* **205**, 2803–2812.
[50] cicco-Skinner KL, Trovato EL, Simmons JK, Lepage PK, and Wiest JS (2011). Loss of tumor progression locus 2 (tpl2) enhances tumorigenesis and inflammation in two-stage skin carcinogenesis. *Oncogene* **30**, 389–397.
[51] Serebrennikova OB, Tsatsanis C, Mao C, Gounaris E, Ren W, Siracusa LD, Eliopoulos AG, Khazaie K, and Tsichlis PN (2012). *Tpl2* ablation promotes intestinal inflammation and tumorigenesis in Apc^{min} mice by inhibiting IL-10 secretion and regulatory T-cell generation. *Proc Natl Acad Sci USA* **109**, E1082–E1091.
[52] Dumitru CD, Ceci JD, Tsatsanis C, Kontoyiannis D, Stamatakis K, Lin JH, Patriotis C, Jenkins NA, Copeland NG, Kollias G, et al. (2000). TNF-α induction by LPS is regulated posttranscriptionally via a Tpl2/ERK-dependent pathway. *Cell* **103**, 1071–1083.

[53] Gantke T, Sriskantharajah S, and Ley SC (2011). Regulation and function of TPL-2, an IκB kinase-regulated MAP kinase kinase kinase. *Cell Res* **21**, 131–145.

[54] Li X, Feng J, Chen S, Peng L, He WW, Qi J, Deng H, and Sun R (2010). Tpl2/AP-1 enhances murine gammaherpesvirus 68 lytic replication. *J Virol* **84**, 1881–1890.

[55] Scaldaferri F, Vetrano S, Sans M, Arena V, Straface G, Stigliano E, Repici A, Sturm A, Malesci A, Panes J, et al. (2009). VEGF-A links angiogenesis and inflammation in inflammatory bowel disease pathogenesis. *Gastroenterology* **136**, 585–595.

[56] Walsh DA and Pearson CI (2001). Angiogenesis in the pathogenesis of inflammatory joint and lung diseases. *Arthritis Res* **3**, 147–153.

[57] Imhof BA and Aurrand-Lions M (2006). Angiogenesis and inflammation face off. *Nat Med* **12**, 171–172.

[58] Jackson JR, Seed MP, Kircher CH, Willoughby DA, and Winkler JD (1997). The codependence of angiogenesis and chronic inflammation. *FASEB J* **11**, 457–465.

[59] Zhang SQ, Yu H, and Zhang LL (2009). Clinical implications of increased lymph vessel density in the lymphatic metastasis of early-stage invasive cervical carcinoma: a clinical immunohistochemical method study. *BMC Cancer* **9**, 64.

[60] Coşkun U, Akyürek N, Dursun A, and Yamaç D (2010). Peritumoral lymphatic microvessel density associated with tumor progression and poor prognosis in gastric carcinoma. *J Surg Res* **164**, 110–115.

[61] Gao J, Knutsen A, Arbman G, Carstensen J, Franlund B, and Sun XF (2009). Clinical and biological significance of angiogenesis and lymphangiogenesis in colorectal cancer. *Dig Liver Dis* **41**, 116–122.

[62] Gao P, Zhou GY, Zhang QH, Xiang L, Zhang SL, Li C, and Sun YL (2008). Clinicopathological significance of peritumoral lymphatic vessel density in gastric carcinoma. *Cancer Lett* **263**, 223–230.

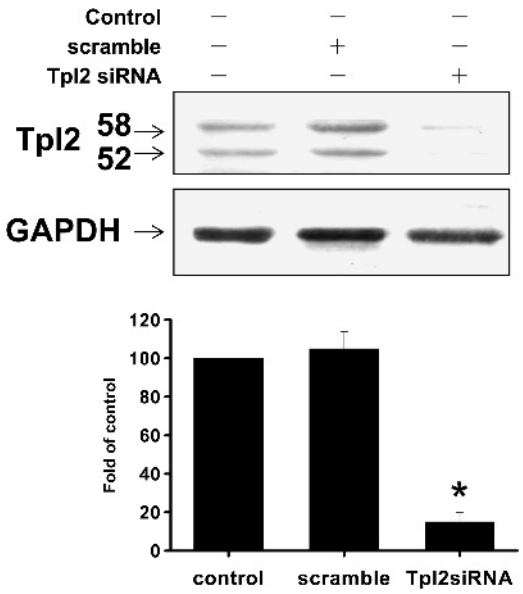

Figure W1. Tpl2 siRNA transfection efficacy detected by Western blot analysis. The efficiency of transfection by Lipofectin reagent (Invitrogen) was determined on the third passage. Transfection of HUVECs with Tpl2 siRNA but not scrambled siRNA caused 85% ablation of Tpl2 protein. Quantification of the protein expression was performed by densitometric analysis (Image-Pro Plus software).

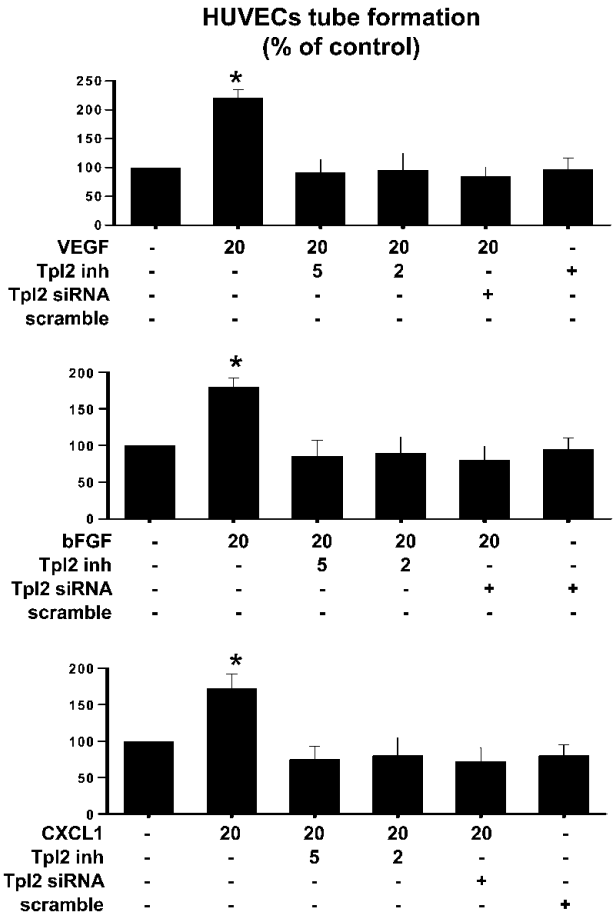

Figure W2. Quantification of HUVEC tube formation.